

Contents lists available at ScienceDirect

Journal of Alloys and Compounds

journal homepage: http://www.elsevier.com/locate/jalcom



Letter

New ultraviolet B emission from gadolinium activated BaZrO₃ phosphor - An electron paramagnetic resonance and optical study



Keywords: Luminescence Inorganic compounds Electron paramagnetic resonance (EPR) Optical properties Photoluminescence spectroscopy

ABSTRACT

Gadolinium activated BaZrO₃ phosphor has been prepared by the solution combustion method. Powder X-ray diffraction and scanning electron microscopy methods are used to characterize the prepared phosphor. Electron paramagnetic resonance (EPR) spectra of un-doped and gadolinium activated BaZrO₃ phosphor has been studied. Pure BaZrO₃ exhibits an EPR spectrum which is a superposition of spectra from two distinct centers. One of the centers (center I) with an isotropic g factor 2.0016 is tentatively assigned to an F⁺ -type center (singly ionized oxygen vacancy). Center II with an axially symmetric g-tensor with principal values $g_{\parallel}=1.955$ and $g_{\perp}=1.973$ is identified as a Zr^{3+} ion. The EPR spectrum of gadolinium activated BaZrO₃ samples exhibit resonance signals with the effective g values at $g\approx 1.94$ and $g\approx 4.10$. The signal at $g\approx 1.94$ has been attributed to Gd^{3+} ions disposed in a weak cubic symmetry field between the Gd^{3+} ion and the phosphor lattice. The excitation spectrum exhibits a dominant band with a maximum at 275 nm (36364 cm⁻¹). Upon excitation at 275 nm (36364 cm⁻¹), the emission spectrum exhibits a well defined ultraviolet B emission band with a maximum at 314 nm (31847 cm⁻¹) corresponding to $^6P_{7/2} \rightarrow ^8S_{7/2}$ transition.

© 2015 Elsevier B.V. All rights reserved.

1. Introduction

In recent years, there is a great interest in the area of luminescence studies of BaZrO₃ doped with rare-earth ions. A few spectroscopic studies have been carried out on BaZrO₃ doped with Tb³⁺, Er³⁺, Eu³⁺ and Pr⁴⁺ ions [1–4]. To the best of our knowledge we are not aware of any study that has been reported regarding the gadolinium doped BaZrO₃ phosphors. Hence the present detailed investigation has been taken up to study the structural and optical properties of gadolinium activated BaZrO₃ phosphors. It is well established that ultraviolet (UV) radiation has been widely used in phototherapy [5–7]. Especially, the narrow band ultraviolet B radiation is used for curing many types of skin disorders. Also gadolinium activated crystallite has attracted considerable research interest owing to its UV emission in a narrow region (300–320) [8]. This narrow region showed remarkable therapeutic effects. The $^6P_I \rightarrow ^8S_{7/2}$ transition of Gd³⁺ is ideal for such emission.

The understanding of perovskite materials is a very active research area of constant interest over the several decades and with great significance to both application and fundamental related issues [9–11]. The general formula ABX₃ belongs to the perovskite family where A and B are cations and X is an anion. It has been reported that in the perovskite oxides structure, the smaller tetravalent B cation resides in the center of corner sharing BO₆ octahedron. And in the ideal case, the larger divalent A cation is located in the cavities between eight octahedron with a 12 fold oxygen

coordination. The perovskite oxide material exhibits a variety of interesting electronic, electromechanical and conductive properties. Especially, BaZrO₃ has high refractive index, high photochemical stability, wide energy gap, and excellent thermal, mechanical, electrical and optical properties [12-15]. In BaZrO₃ tetravalent cation fits almost perfectly on the B-site. It should be noted that Goldschmidt tolerance factor is about one and the symmetry of these materials is cubic [16]. Bilic and Gale [17] investigated ground state properties of BaZrO₃ using density-functional theory calculations. Theoretical and experimental study of BaZrO₃ was carried out at low temperature by Akbarzadeh et al. [18]. Gomez et al. [19] studied the effect of yttrium dopant on the proton conduction pathways of BaZrO₃, a cubic perovskite material. A simple hydrothermal method was adopted to prepare nanocrystalline BaZrO3:Yb, Tm and the size, morphology, band gap, and photoluminescence of the oxide particles were investigated [20]. Mohanta and Behera [21] studied magnetic field dependence of the pinning effect in BaZrO₃ doped Y-Ba-Cu superconductor. Moreira et al. [22] studied radioluminescence properties of deca-octahedral BaZrO₃ nano-crystals. Several investigations have been carried out [23-30] on BaZrO₃ to obtain structural information using various spectroscopic methods. As far as we know, there are no previous reports on gadolinium activated BaZrO₃ phosphors. In view of this, a detailed investigation on gadolinium activated BaZrO₃ phosphors has been undertaken using spectroscopic methods such as X-ray diffraction (XRD), scanning electron microscopy (SEM), electron paramagnetic

resonance (EPR) and optical studies.

2. Materials preparation and analysis

Gd activated BaZrO $_3$ was prepared utilizing the combustion synthesis methods. In a typical synthesis 1.9557 g of Ba(NO $_3$) $_3$, 2.00 g of ZrO(NO $_3$) $_2$ · 2H $_2$ O, 0.1013 g of Gd(NO $_3$) $_3$ · 6H $_2$ O and 2.40 g of NH $_2$ CONH $_2$ were dissolved in a minimum quantity of deionized water in a China dish of 300 ml capacity. The solution was allowed to react at 80 °C for 30 min to obtain a homogenous solution. Then the dish was introduced into a muffle furnace preheated to 550 °C. The water quickly evaporated and the mixture formed foam, within which a vigorous reaction between the nitrates and urea soon initiated and ended. The entire combustion process was completed in about 3–5 min. The resulting white fluffy masses were crushed into a fine powder. Then the powder was transferred to a 50 ml alumina crucible to be heat-treated at 1100 °C for 3 h in air to remove by-products and reduce internal strains before it was used for the further characterization.

Powder XRD pattern was recorded in the 2θ range from 5° to 80° on a Philips X'Pert X-ray diffractometer with graphite monochromatized CuK $_{\alpha}$ radiation and nickel filter at a scanning step of 0.3°. Powder morphology was studied using Scanning electron microscopy (Hitachi S-3200N, Japan). Absorption spectroscopy was performed at room temperature by diffuse reflectance with a Cary 6000i UV-Vis-NIR absorption spectrophotometer. A powdered sample of 100 mg is taken in a quartz tube for the EPR measurements. The EPR spectra of the sample were recorded on a JEOL FE1X ESR Spectrometer, operating in the X-band frequencies, with a field modulation of 100 kHz. Emission and excitation spectra were recorded using a Fluorolog 3—22 spectrometer (Jobin Yvon) with a 450W Xenon lamp as an excitation source.

3. Results and discussion

3.1. XRD phase analysis

Fig. 1 shows the XRD pattern of the BaZrO₃:Gd³⁺ phosphor powder. The observed diffraction peaks in the recorded XRD pattern correspond to those of the standard pattern for BaZrO₃ (JCPDS, No. 74-1299). All signals on the pattern can be indexed to pure cubic crystal structure of BaZrO₃. The diffraction pattern indicates that doping with gadolinium ions has negligible effect on the crystal structure of BaZrO₃. As indicated by XRD pattern, crystallinity and cubic phase of BaZrO₃ could be obtained by the solution combustion synthesis.

3.2. Morphological analysis

Scanning electron microscopy study was carried out to investigate the morphology of the synthesized phosphor powder. Fig. 2 displays SEM images of the BaZrO₃:Gd³⁺ phosphors that are taken at various magnifications. SEM image is shown in Fig. 2(A) and the image indicates that the powder particles are highly agglomerated with rough surface and also has pores, voids and cracks. It is also clearly seen that the particles are non-uniform and irregular in shape and sizes. The non-uniform and irregular behavior of the

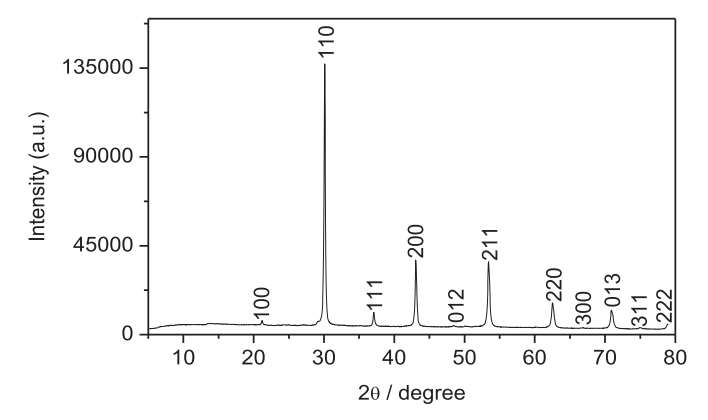


Fig. 1. Powder XRD pattern of BaZrO₃:Gd³⁺ phosphor.

particles can be attributed to the non-uniform distribution of temperature and mass flow in the combustion flame. A magnified portion of Fig. 2A (portion a) is shown in Fig. 2B. Portion (a') of Fig. 2A is magnified to obtain Fig. 2C. When a gas is escaping under high pressure, pores, voids and cracks are formed with the formation of small particles, and this is clearly illustrated by Fig. 2B and C. Portion (b) of Fig. 2B is magnified to obtain Fig. 2D and portion (c) of Fig. 2C is magnified to obtain Fig. 2E. These higher magnification images (Fig. 2C, D & E) show that the particles are interconnected, which is a characteristic of the combustion product.

3.3. Electron paramagnetic resonance studies

EPR spectrum of pure BaZrO₃ sample was recorded at room temperature (RT) and 123 K. The room temperature spectrum recorded in the free-electron region ($g_e \approx 2.0023$) is shown in Fig. 3(a) and the low field spectrum is displayed in Fig. 3(b). The spectrum exhibits sharp and intense signals in the free-electron region and also at $g \approx 4.03$ and a small broad signal at $g \approx 7.50$. The signals at $g \approx 4.03$ and 7.50 may be attributed to unintentional Fe³⁺ impurity which is present in the starting chemicals [31]. The chemicals have been found to contain 10–30 ppm Fe impurity. It is inferred that the observed spectrum in the 3470 G magnetic field region ($g \approx 2$) arises from two distinct centers. The EPR lines associated with these centers are labeled in Fig. 3(a).

BaZrO₃ belongs to the ABO₃ family of perovskites and has a cubic symmetry structure with space group Pm3m [32]. The unit cell has the parameters a=b=c=0.4193 nm. Zr ions are surrounded by regular octahedron of oxygens which are linked together by their corners to form a three-dimensional framework. Barium cations are in a 12-fold cuboctahedral coordination.

In BaZrO₃, Ba site may be expected to have mixed occupancy with partial replacement by Zr atoms. Substitution of this kind arising from antisite cation exchange or the cation exchange disorder is a point defect in crystal lattices wherein cations exchange positions. The concentration and distribution of these defects in crystal lattices influence the electrical conductivity, optical properties, ionic diffusion, and the resulting chemical properties. Theoretical calculations have predicted the presence of such defects [33] and confirmed by X-ray diffraction [34], X-ray absorption fine structure [35] and direct observation by advanced electron microscopy [36]. An example of the effect of cation exchange disorder on the luminescence properties is provided by a recent study of Cr³⁺ doped AB₂O₄ spinel compounds [37].

In BaZrO₃, a number of trapping sites for the electron and hole may be created due to antisite formation which results from the interchange of the ions in the octahedral and cuboctahedral positions by divalent and tetravalent ions. The line labeled as I in Fig. 3(a) is due to a center characterized by an isotropic g-value equal to 2.0016 and 20 G linewidth. The EPR line is broad and indicates a possible unresolved hyperfine structure. The unresolved structure results from the interaction of the unpaired electron with nearby nuclear spins. Barium has isotopes with nuclear spin 3/2: ¹³⁵Ba and ¹³⁷Ba. ¹³⁷Ba is more abundant (11.2%) than ¹³⁵Ba (6.6%) and its nuclear magnetic moment (0.94) is higher than that of ¹³⁵Ba (0.84). Zirconium isotope ⁹¹Zr has a nuclear spin 5/2. It is 11.2% abundant with a magnetic moment –1.30 [38]. It is likely, therefore, that the electron spin will be interacting with barium ions and also possibly with zirconium ions.

In oxide systems, disorder of cations and non-stoichiometry can give rise to lattice defects which may serve as trapping centers. First principle calculations have shown that oxygen vacancies would more easily form with cation disorder than in a perfect cation-ordered system [39]. Such vacancies can trap electrons and result in the formation of F⁺ -centers. One of the probable centers which

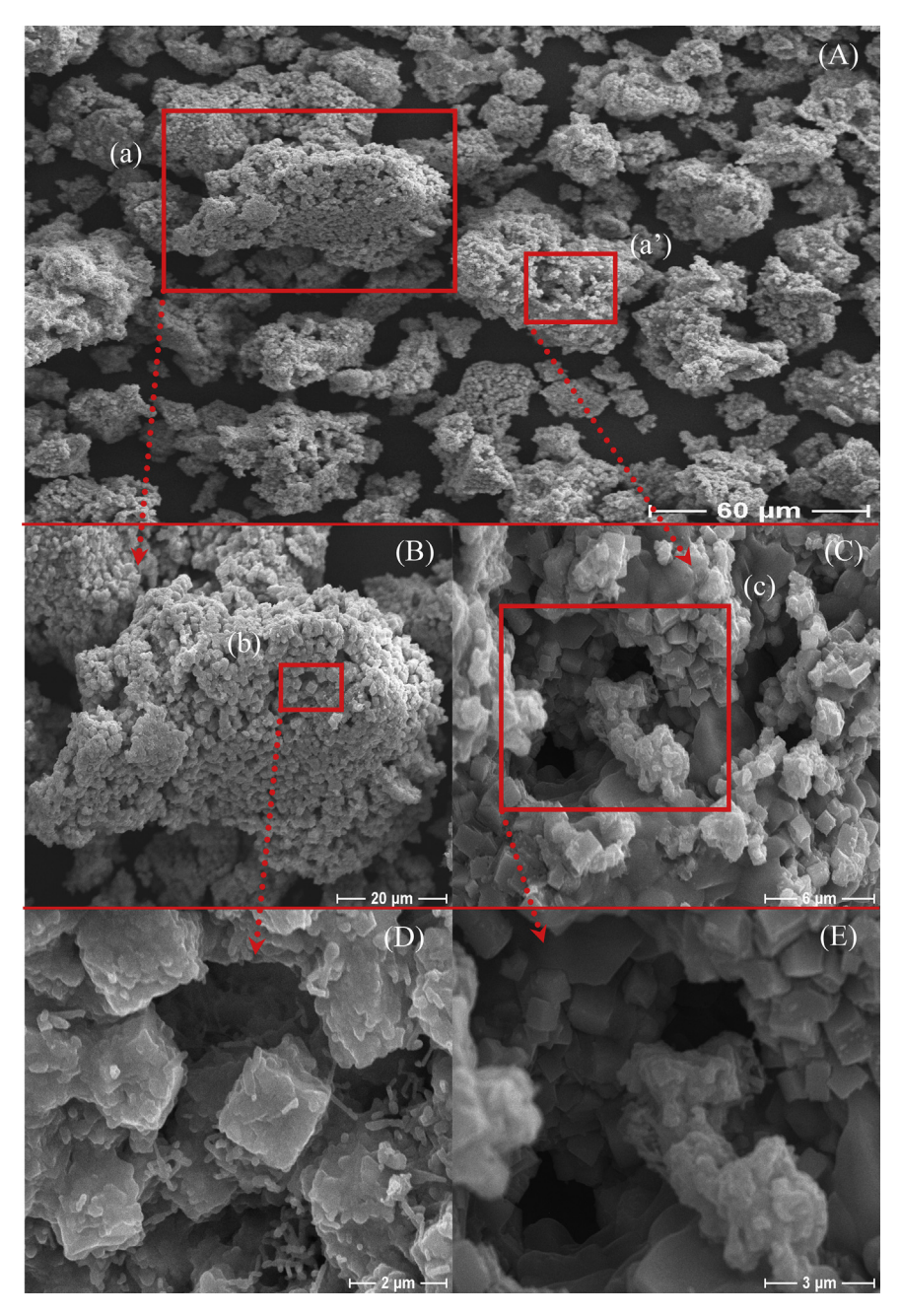


Fig. 2. SEM micrographs of BaZrO₃:Gd³⁺ phosphor.

is likely to be formed in BaZrO $_3$ is an F $^+$ -center (an electron trapped at an anion vacancy). The earliest observation of this center was in neutron irradiated LiF [40]. In LiF, a single broad line (linewidth ≈ 100 G) with a g-factor equal to 2.008 was observed. The inherent linewidth of F $^+$ -center is approximately 1 G (as observed in MgO system [41]). The ions present in a system determine the experimentally observed linewidth (whether they have nuclei with magnetic moment and their abundance) and also on the amount of delocalization of the unpaired electron which depends on the host lattice. An unusually large linewidth is observed in alkali halides as the electron is delocalized and interacts with several alkali and halide ions from successive neighboring shells. In KCl, the observed line width is approximately 20 G [42] and in LiCl it is 58 G [42]. In other systems like HgI $_2$.2HgS [43] and BaO [44], the linewidths are about 10 G and 3.5 G respectively. In

general, a variation in linewidth is observed. Small g-shifts, which may be positive or negative, are the normal feature of F⁺-centers. Further they are characterized by linewidths which depend on the host lattice. An anionic vacancy can trap an electron during irradiation or synthesis of the phosphor and such trapping is the basis for the formation of F⁺-centers. Large linewidths can arise from hyperfine interaction with the nearest-neighbor cations. Center I formed in the present system is characterized by a small g-shift. The center does not exhibit hyperfine structure but the linewidth is relatively large. A recent report of observation of such a center is in LiAlO₂ and ZnAl₂O₄ phosphors [45,46]. Based on these observations and considering the likely defect centers that can form in BaZrO₃, center I is tentatively assigned to an F⁺-center. It is to be mentioned that F⁺-centers are normally formed due to irradiation by ionizing radiations. The present system appears to be a rare case

-1200

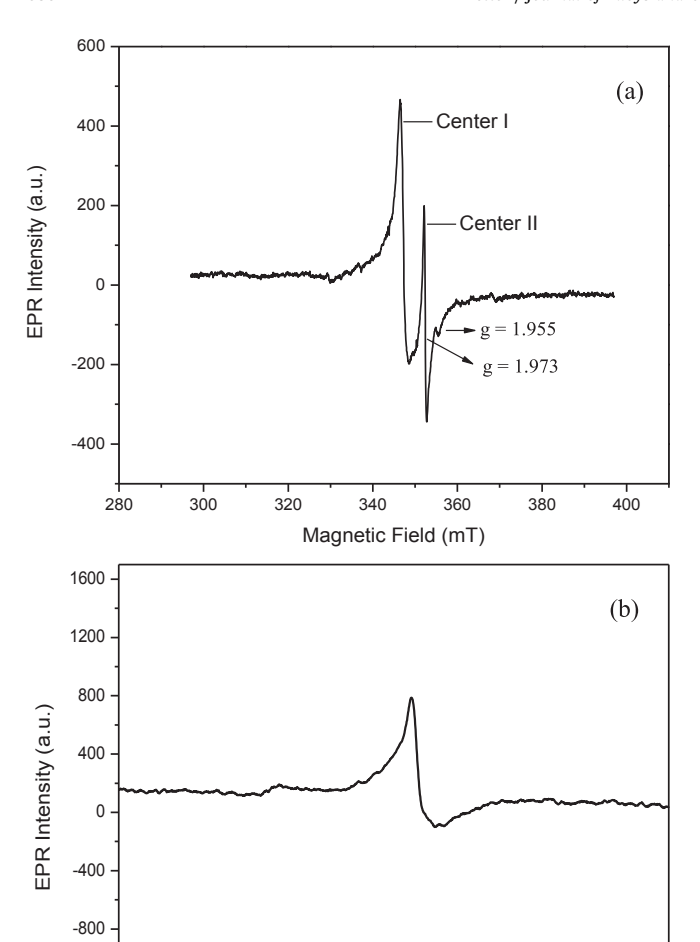


Fig. 3. Room temperature EPR spectrum of BaZrO₃ spectrum (a) recorded in the free-electron region ($g_e \approx 2.0023$). Center I line is assigned to an F⁺-center and center II characterized by an axial g-tensor is attributed to a Zr ³⁺ ion and (b) Room temperature EPR spectrum of BaZrO₃ spectrum recorded in the low field region. The observed lines at $g \approx 4.03$ and 7.50 are due to Fe³⁺ ion.

150

Magnetic Field (mT)

200

250

100

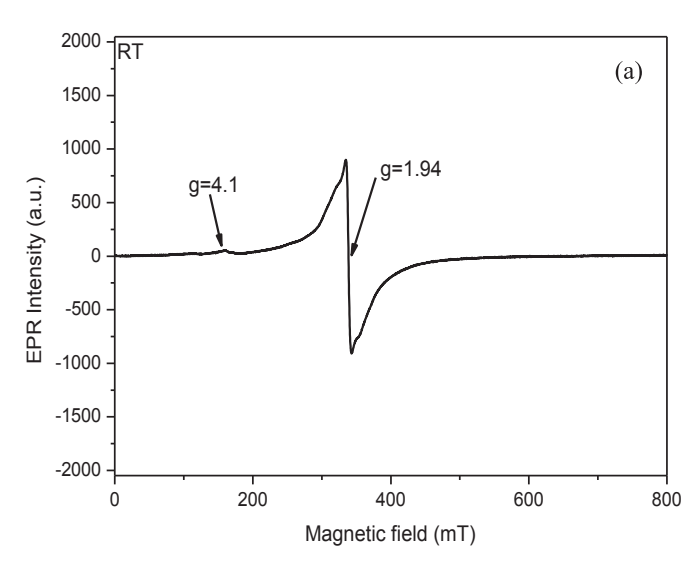
50

where such centers are formed during synthesis procedures. Though rare, there are reports of detection of F^+ -centers in oxide systems which are not subjected to ionizing radiation and observed in as prepared pristine samples. For example, in yttrium—aluminum perovskite YAlO_3 single crystals grown in vacuum, Zorenko et al. [47] reported the detection of F^+ -centers in their photoluminescence studies of $Al_2O_3-Y_2O_3$ oxide system. In recent years, F^+ -center has been identified in nanocrystalline MgO using photoluminescence spectra [48] while an intense ESR signal (g~2.003) observed in air and vacuum annealed TiO_2 nanoparticles has been assigned to an F^+ -center [49].

Center II shown in Fig. 3(a) does not exhibit any hyperfine structure and is characterized by an axially symmetric g-tensor with principal values $g_{\parallel}=1.955$ and $g_{\perp}=1.973$. In a recent study of defects formed in polycrystalline pristine Zirconia and those formed after reductive treatments of Zirconia, Gionco et al. [50] reported the observation of Zr^{3+} ions. EPR studies have shown that one of the ions is characterized by the principal g-values $g_{\perp}=1.9768$ and $g_{\parallel}=1.9589$. Several studies have also reported Zr^{3+} ion which has a d^{I} configuration viz., polycrystalline ZrF_{4} [51], Zr doped YAG [52], Zr doped YPO₄ and $ScPO_{4}$ [53] and nuclear glasses [54]. The

ion is in lower symmetry environment in these systems such as being in sixfold, sevenfold or eightfold coordinated sites. These studies show that the g-value of the ion in a distorted cube or in a distorted octahedral are less than the free-electron value (ge ~2.0023) and also $g_{\parallel} < g_{\perp}$. The g-values have been interpreted in terms of crystal field theory which gives $g_{\perp} \sim g_e$ and $(g_{\parallel} - g_e) \sim -\lambda/\Delta$ where Δ is the splitting between the cubic crystal field E and T_2 levels and λ the spin—orbit coupling constant (for Zr^{3+} ion λ ~500 cm $^{-1}$) [55]. Essentially the g-shifts depend on the ratio between the spin—orbit coupling of the Zr ion and the crystal field splitting [56].

Based on these results and observations, center II with an axial nature of the g-tensor and with negative g-shifts and relatively large anisotropy in g-values in the present system $BaZrO_3$ is tentatively ascribed to Zr^{3+} ion. The axial nature of the g-tensor arises from a Zr^{3+} ion being present in a site that deviates from a regular octahedral environment. In $BaZrO_3$ with an ideal perovskite structure, Zr ion is located at a site of regular octahedron environment provided by oxygens. The presence of oxygen vacancies in the lattice due to antisite disorder causes a rearrangement of the nearest-neighbor oxygens to Zr ion. The resulting deviation from regular octahedral environment leads to the axial nature of the g-tensor.



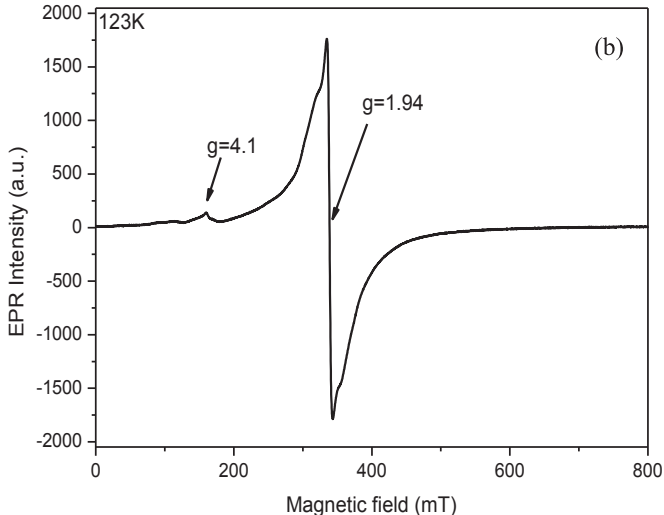


Fig. 4. EPR spectrum of $BaZrO_3$: Gd^{3+} phosphor at (a) room temperature and (b) at 123 K.

The room temperature EPR spectrum of BaZrO₃:Gd³⁺ phosphor is shown in Fig. 4(a). This spectrum exhibits signals at $g \approx 1.94$ and 4.10. The signal at $g \approx 1.94$ is attributed to Gd³⁺ ions in a weak crystal field between the dopant and the lattice [57]. The signal at $g \approx 4.10$ might be due to unintentional Fe³⁺ impurity ions. Fig. 4(b) shows the EPR spectrum of BaZrO₃:Gd³⁺ phosphor observed at 123 K. Similar to room temperature EPR spectrum, 123 K EPR spectrum exhibits signals at $g \approx 1.94$ and $g \approx 4.10$. The intensity of the resonance signals increases with decreasing temperature in accordance with the Boltzmann law. The g values are independent of temperature variation, suggesting that the structural environment is invariant between Gd³⁺ and the phosphor lattice.

The electronic configuration of Gd^{3+} ion is [Xe]4 f^7 and the spin quantum number S is 7/2 and the ground state is $^8S_{7/2}$. With the orbital angular momentum L=0 in crystals, a crystalline field alone can't split an S state. Higher order perturbations involving spin—orbit coupling and spin—spin coupling lead to splitting. The strong spin—orbit coupling of 4f electrons breaks the L-S scheme of energy levels and the ground multiplet is mixed with $L\neq 0$ states which results in large crystal field interactions. In this situation, the EPR spectrum of Gd^{3+} ion is characterized by several lines dependent on the local symmetry of Gd^{3+} ion and the magnitude of crystal field interaction.

The powder EPR spectrum of Gd ion has been classified by Brodbek and Iton [58] on the basis of the magnitude of crystal field interaction (H_{CF}) in relation to the Zeeman splitting which is measured by hy (where y is the microwave frequency). They consider the EPR spectra in three regions which depend on the ratio H_{CF}/hv viz., weak, intermediate and strong. In the weak crystal field region, $H_{CF}/h\nu < \frac{1}{4}$ and the spectra are primarily in the g = 2.0 region and higher order transitions are forbidden. Intermediate CF region has been considered in two parts; (a) lower intermediate and higher intermediate CF regions. In the lower intermediate region $(\frac{1}{4} \le H_{CF}/h\nu \le 1)$, EPR spectrum will be observed over a wide region where g varies over the values $2.0 < g < \infty$. For the case of higher intermediate CF region, a group of resonances with g > 2.0 is expected. In the strong CF case $(H_{CF}/h\nu \ge 4)$, the EPR spectrum is entirely controlled by the resonances resulting from transitions within the Kramer's levels.

The ionic radius of Ba^{2+} ion is 1.61 Å in a 12-fold coordination and ${\rm Zr}^{4+}$ ion has 0.72 Å radius in an octahedral coordination (6fold) [59]. Gd³⁺ with an ionic radius of 0.94 Å in a 6-fold coordination is likely to be located at the 6-fold coordinated Zr⁴⁺ sites on the basis of ionic radii considerations. Gd3+ ion has a higher ionic radius in case it is located at a site with higher coordination number. For example, the ionic radius is 1.11 Å in a 9-fold coordination. In a previous study on $BaMO_3$ (M = Ce, Zr, Sn) host materials, the rare-earth ion Pr⁴⁺ (0.85 Å ionic radius in a 6-fold coordination) is observed to be substituted for M⁴⁺ ions i.e., it is in an octahedral site [60]. On the other hand, it is also reported that Gd³⁺ replaces Ba ions in the perovskite BaTiO₃ crystal [61], a system similar to the present BaZrO₃. Therefore, there exists a possibility that in BaZrO₃, Gd³⁺ ion may replace Ba ions as well as Zr ions. The EPR spectrum appears to result from a superposition of two lines of differing linewidths but with almost similar g-values. The narrow line has 86 G linewidth while the broader line has 296 G linewidth and the gvalue is 1.94. The two lines are tentatively interpreted as arising

from Gd³⁺ ions located at Ba²⁺ and Zr⁴⁺ sites.

A replacement of Ba²⁺ ions by Gd³⁺ requires charge compensation to take care of the excess charge of the Gd³⁺ ion. This can be achieved by creation of Ba²⁺ vacancies. If the vacancy is near the Gd³⁺ ion, the charge compensator is likely to alter the normal symmetry of the substitutional site. If a distortion occurs in the environment of Gd³⁺ ion, then it is possible that the crystal field seen by the

 Gd^{3+} ion will increase. This will lead to the appearance of EPR lines in the low field region which is expected in the case of intermediate crystal fields [58]. The lines seen only near g=2.0 in the present case indicate that for most of the Gd^{3+} ions the charge compensator is at a remote location and the local symmetry is not perturbed by the charge compensator. It is to be noted that the incorporation of Gd^{3+} ions at the Zr^{4+} sites also requires charge compensation by way of creation of anion vacancies.

3.4. Optical studies

The diffuse reflectance spectrum of BaZrO₃:Gd³⁺ phosphor observed at room temperature is shown in Fig. 5. This spectrum presents a weak band at \approx 319 nm (31348 cm⁻¹) and a broad band at low energy side at \approx 1417 nm (7057 cm⁻¹). The band at \approx 1417 nm (7057 cm⁻¹) is difficult to assign [52, 62]. The band at about 319 nm (31348 cm⁻¹) has been attributed to defect level in host. In the case of Gd³⁺ ions, the first excited state occurs at above 32000 cm⁻¹ from the ground state. Due to this fact, perhaps the band at \approx 319 nm (31348 cm⁻¹) is not due to Gd³⁺ ions but due to defect level in host.

Room temperature photoluminescence spectra of BaZrO₃:Gd³⁺ phosphor is shown in Fig. 6. Fig. 6(a) and (b) shows the excitation and emission spectra of BaZrO₃:Gd³⁺ phosphor, respectively. The excitation spectrum exhibits two very weak bands at ≈ 248 , 254 nm (40323, 39370 cm $^{-1}$) and prominent bands with maxima at ≈ 275 , 276.5 nm (36364, 36166 cm $^{-1}$) in the UV region when emission wavelength is fixed at 314 nm (31847 cm $^{-1}$). The former bands due to the $^8{\rm S}_{7/2} \rightarrow ^6{\rm D}_J$, and the latter bands due to the $^8{\rm S}_{7/2} \rightarrow ^6{\rm D}_J$ transitions of Gd $^{3+}$ ions. The observed bands are related to the f—f transitions of Gd $^{3+}$ ions. The observed band positions and their assignments are in good agreement with the band positions reported elsewhere [63]. Singh et al. [64] reported luminescence and EPR investigation on ultraviolet emitting Gd doped MgAl₂O₄ phosphors. They observed five bands at 246, 253, 273, 276 and 279 nm in the excitation spectrum when the emission is fixed at 312 nm.

Gd³⁺ ion belongs to 4f⁷ electronic configuration. The energy gap between the ground state and the first excited state is approximately 32000 cm⁻¹. Theoretical calculations show that the 4f⁷ energy levels of Gd³⁺ ions can extend up to 150000 cm⁻¹. The energy levels up to 67000 cm⁻¹ have been reported experimentally [65]. Studies of Gd³⁺ ions in phosphors is limited because of strong absorption in phosphor lattice in the UV region which masks all the absorption bands except from a few low lying excited states. Fig. 6(b) shows the emission spectrum of BaZrO₃:Gd³⁺ phosphor observed when the excitation wavelength is fixed at 275 nm

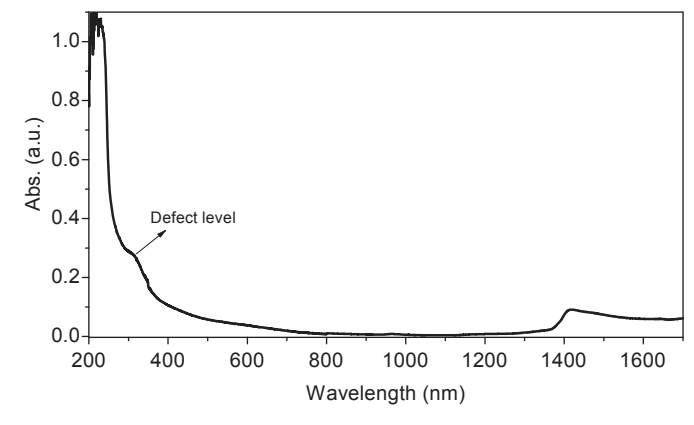
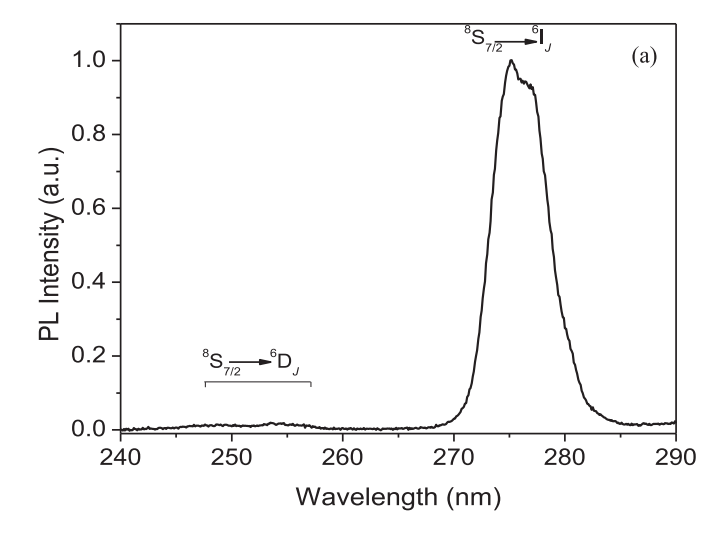


Fig. 5. Diffuse reflectance spectrum of BaZrO₃:Gd³⁺ phosphor.



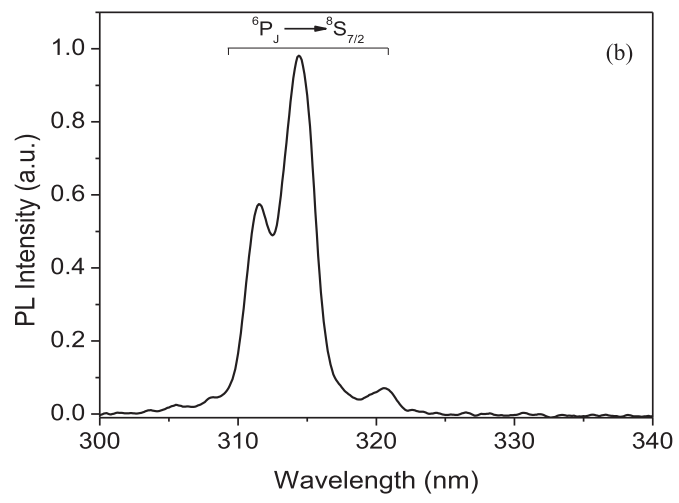


Fig. 6. Photoluminescence spectra of BaZrO₃ phosphor (a) Excitation spectrum of $BaZrO_3:Gd^{3+}$ ($\lambda_{em}=314$ nm) and (b) Emission spectrum of $BaZrO_3:Gd^{3+}$ $(\lambda_{ex} = 275 \text{ nm}).$

(36364 cm⁻¹). This spectrum exhibits a prominent band at \approx 314 nm (31847 cm⁻¹), a relatively prominent band at \approx 311.5 nm (32103 cm⁻¹) and a weak band at \approx 320.6 nm (31192 cm⁻¹). These bands result from transition between the excited state (⁶P_I) and ground state (⁸S_{7/2}) of Gd³⁺. This emission is classified as ultraviolet B (UVB) and it is suitable for use in phototherapy lamps to treat various skin diseases. The observed band positions are in good agreement with the band positions reported in literature [63]. Singh et al. [66] observed an emission band at 313 nm in $Gd_2Zr_2O_7$ phosphor and was assigned to ${}^6P_{7/2} \rightarrow {}^8S_{7/2}$ transition. Also, they [64] observed an emission band at about 312 nm in the emission spectrum of Gd doped MgAl₂O₄ phosphor. The band at \approx 320.6 nm (31192 cm⁻¹) is a phonon assisted band and has been attributed to $^6P_{7/2} \rightarrow ^8S_{7/2}$ transition. Parrish and Jacnicke [67] conducted phototherapy investigations in the UV (270–320 nm) region. They found UV emission in a narrow region 300-320 nm displayed significant therapeutic effects and the UV emission in the region 270-300 nm is not much operative and even leads to side effects. As per the present investigation, the obtained photoluminescence results have indicated that the prepared phosphor with a narrow band centered at ≈ 314 nm (31847 cm⁻¹) could be a potential candidate for phototherapy application.

4. Conclusions

Gadolinium activated BaZrO₃ powder is successfully prepared by urea combustion method. The XRD pattern of prepared phosphor powder exhibits a pure cubic crystal structure. Two centers have been identified in pure BaZrO₃ based on EPR studies. These centers are tentatively assigned to an F⁺ center and Zr³⁺ ion. The two overlapping resonance signals at $g \approx 1.94$ in the Gd doped phosphor are attributed to Gd³⁺ ion located at the Ba and Zr sites in the lattice. The resonance signal at $g \approx 4.1$ might be due to Fe³⁺ ion impurity in the sample. The g values are independent of temperature variation. The observed major narrow UV emission band at \approx 314 nm (31847 cm⁻¹) corresponds to the transition $^6P_I \rightarrow ^8S_{7/2}$. The UV emission makes BaZrO₃:Gd³⁺ phosphor a good candidate for applications in phototherapy lamps.

Acknowledgments

This paper was supported by the KU Research Professor Program of Konkuk University. T. K. Gundu Rao is grateful to CAPES, Brazil for the research fellowship.

References

- [1] B. Mari, K.C. Singh, M. Sahal, S.P. Khatkar, V.B. Taxak, M. Kumar, J. Lumin. 130
- [2] L. Guo, C. Zhong, X. Wang, L. Li, J. Alloys Compd. 530 (2012) 22.
- X. Liu, X. Wang, Opt. Mater. 30 (2007) 626.
- [4] Y. Hinatsu, N. Edelstein, J. Alloys Compd. 250 (1997) 400.
- [5] R.P. Sinha, D.P. Häder, Photochem. Photobiol. Sci. 1 (2002) 225.
- [6] W.L. Morison, Semin. Cutan. Med. Surg. 18 (1999) 297.
- H. Honingsmann, Clin. Exp. Dermatol. 26 (2001) 343.
- [8] D.S. Thakare, S.K. Omanwar, P.L. Muthal, S.M. Dhopte, V.K. Kondawar, S.V. Moharil, Phys. Stat. Sol. 201 (2004) 574.
- [9] H. Iwahara, Y. Asakura, K. Katahira, M. Tanaka, Solid State Ionics 168 (2004)
- [10] P.M. Woodward, Acta Cryst. B 53 (1997) 44.
- V. Ravi, T.R.N. Kutty, Mater. Sci. Eng. B 10 (1991) 41.
- [12] J.W. Bennett, I. Grinberg, A.M. Rappe, Phys. Rev. B 79 (2009) 235115.
- [13] F. Boschini, A. Rulmont, R. Cloots, B. Vertruyen, J. Eur. Ceram. Soc. 29 (2009)
- [14] X.X. Chen, L. Rieth, M.S. Miller, F. Solzbacher, Sens. Actuators B Chem. 137 (2009) 578.
- [15] S.B.C. Duval, P. Holtapples, U.F. Vogt, U. Stimming, T. Graule, Fuel Cells 9 (2009) 613.
- [16] P. Goudochnikov, A.J. Bell, J. Phys. Condense. Matter 19 (2007) 176201.
- [17] A. Bilic, J.D. Gale, Phys. Rev. B 79 (2009) 174107.
- [18] A.R. Akbarzadeh, I. Kornev, C. Malibert, L. Bellaiche, J.M. Kiat, Phys. Rev. B 72 (2005) 205104.
- [19] M.A. Gomez, M. Chunduru, L. Chigweshe, L. Foster, S.J. Fensin, K.M. Fletcher, L.E. Fernandez, J. Chem. Phys. 132 (2010) 214709.
- [20] R. Borja-Urby, L.A. Diaz-Torres, P. Salas, M. Vega-Gonzalez, C. Angeles-Chavez, Mater. Sci. Eng. B 174 (2010) 169.
- [21] A. Mohanta, D. Behera, Solid State Commun. 150 (2010) 1325.
- [22] M.L. Moreira, D.P. Volanti, J. Andres, P.J.R. Montes, M.E.G. Valerio, J.A. Varela, E. Longo, Scr. Mater. 64 (2011) 118.
- [23] X.X. Chen, L. Rieth, M.S. Miller, F. Solzbacher, Sens. Actuators B Chem. 148 (2010) 173.
- [24] D.Y. Gao, R.S. Guo, Mater, Lett. 64 (2010) 573.
- F. Gionnici, A. Longo, K. Kreuer, A. Balerna, A. Martorana, Solid State Ionics 181 (2010)122
- [26] C. Laulhe, A. Pasturel, F. Hippert, J. Kreisel, Phys. Rev. B 82 (2010) 132102.
- [27] F. Gionnici, A. Longo, A. Balerna, K. Kreuer, A. Martorana, Chem. Mater. 21 (2009) 2641.
- [28] J. Park, J. Lee, H. Lee, B. Kim, Solid State Ionics 181 (2010) 163.
- [29] C. Peng, J. Melnik, J. Luo, A.R. Sanger, K.T. Chuang, Solid State Ionics 181 (2010)
- [30] J. Tong, D. Clark, M. Hoban, R. O'Hayre, Solid State Ionics 181 (2010) 496.[31] C. Moon, M. Nishi, K. Miura, K. Hirao, J. Lumin 129 (2009) 817.
- [32] H.D. Megaw, Proc. Phys. Soc. London 58 (1946) 133.
- [33] M.M. Kuklja, J. Phys. Condens. Matter 12 (2000) 2953
- [34] A.P. Patel, M.R. Levy, R.W. Grimes, R.M. Gaume, R.S. Frigelson, K.J. McClellan, C.R. Stanek, Appl. Phys. Lett. 93 (2008) 191902.
- J. Dong, K. Lu, Phys. Rev. 43 (1991) 8808.
- D. Truong, M.K. Devaraju, T. Tomai, I. Honma, ACS Appl. Mater. Interfaces 5 2013) 9926.
- [37] N. Basavaraju, K.R. Priolkar, D. Gourier, S.K. Sharma, A. Bessiere, B. Viana, Phys.

Chem. Chem. Phys. 17 (2015) 1790.

- [38] R.C. Weast (Ed.), Handbook of Chemistry and Physics, CRC, Cleveland, 1971.
- [39] N. Yuan, X. Liu, F. Meng, D. Zhou, J. Meng, Ionics 21 (2015) 1675.
- [40] C.A. Hutchison, Phys. Rev. 75 (1949) 1769.
- [41] J.E. Wertz, P. Auzins, R.A. Weeks, R.H. Silsbee, Phys. Rev. 107 (1957) 1535.
- [42] W.C. Holton, H. Blum, Phys. Rev. 125 (1962) 89.
- [43] K. Takei, H. Hagiwara, H. Tanaka, Bull. Chem. Soc. Jpn. 50 (1977) 1341.
- [44] A.J. Tench, R.L. Nelson, Proc. Phys. Soc. 92 (1967) 1055.
- [45] B. Dhabekar, E. Alagu Raja, S. Menon, T.K. Gundu Rao, R.K. Kher, B.C. Bhatt, Rad. Meas. 43 (2008) 291.
- [46] S. Menon, B. Dhabekar, E. Alagu Raja, S.P. More, T.K. Gundu Rao, R.K. Kher, J. Lumin, 128 (2008) 1673.
- [47] Yu V. Zorenko, A.S. Voloshinovski, I.V. Konstankevych, Opt. Spectrosc. 96 (2004) 532.
- [48] B. Choudhury, P. Basyach, A. Choudhury, J. Lumin. 149 (2014) 280.
- [49] B. Choudhury, A. Choudhury, Sci. Adv. Mater. 6 (2014) 2115.
- [50] C. Gionco, M.C. Paganini, E. Giamello, R. Burgess, C. Di Valentin, G. Pacchioni, Chem. Mater. 25 (2013) 2243.
- [51] R. Cases, D.L. Griscom, D.C. Tran, J. Non Cryst. Solids 72 (1985) 51.
- [52] G.R. Asatryan, A.S. Kuzanyan, A.G. Petrosyan, A.K. Petrosyan, E.G. Sharoyan, Sov. Phys. Solid. State 27 (1985) 2073.
- [53] M.M. Abraham, L.A. Boatner, J.O. Ramey, M. Rappaz, J. Chem. Phys. 81 (1984) 5362.
- [54] B. Boizot, G. Petite, D. Ghaleb, G. Calas, Nucl. Instr. Meth., B 141 (1991) 580.
- [55] O.M. Orera, R.I. Merino, Y. Chen, R. Cases, P.J. Alonso, Phys. Rev. B 42 (1990) 9782.
- [56] A. Abragam, B. Bleany, Electron Paramagnetic Resonance of Transition Ions, Oxford University, New York, 1970, p. 456.
- [57] Vijay Singh, R.P.S. Chakradhar, J.L. Rao, Isabelle Ledoux-Rak, Ho-Young Kwak, J. Mater. Sci. 46 (2011) 1038.
- [58] C.M. Brodbeck, L.E. Iton, J. Chem. Phys. 83 (1985) 4285.
- [59] R.D. Shannon, Acta Cryst. A32 (1976) 751.
- [60] Y. Hinatsu, J. Solid State Chem. 122 (1996) 384.
- [61] I. Rimai, G.A. deMars, Phys. Rev. 148 (1966) 317.
- [62] W.C. Zheng, Physica B 215 (1995) 255.
- [63] W.T. Carnall, P.R. Fields, K. Rajnak, J. Chem. Phys. 49 (1968) 4443.
- [64] Vijay Singh, G. Sivaramaiah, J.L. Rao, S.H. Kim, J. Lumin. 143 (2013) 162.
- [65] R.T. Wegh, H. Donker, A. Meijerink, Phys. Rev. B 56 (1997) 13841.

- [66] Vijay Singh, G. Sivaramaiah, J.L. Rao, S.H. Kim, Physica B 416 (2013) 101.
- [67] J.A. Parrish, K.F. Jacnicke, J. Invest. Dermatol 76 (1981) 359.

Vijay Singh^{*}

Department of Chemical Engineering, Konkuk University, Seoul 143-701, Republic of Korea

G. Sivaramaiah

Department of Physics, Government College (M), Kadapa 516004, India

J.L. Rao

Department of Physics, Sri Venkateswara University, Tirupati 517 502, India

S. Watanabe, T.K.Gundu Rao

Institute of Physics, University of Sao Paulo, SP 05508-090, Brazil

Sujit S. Jagtap

Department of Chemical Engineering, Konkuk University, Seoul 143-701, Korea

P.K. Singh

Materials Research Laboratory, Sharda University, Greater Noida 201310, India

* Corresponding author.

E-mail address: vijayjiin2006@yahoo.com (V. Singh).

22 May 2015

Available online 4 July 2015